14

Near-Field Scanning Optical Microscopy in Cell Biology and Cytogenetics

Michael Hausmann, Birgit Perner, Alexander Rapp, Leo Wollweber, Harry Scherthan, and Karl-Otto Greulich

Summary

Light microscopy has proven to be one of the most versatile analytical tools in cell biology and cytogenetics. The growing spectrum of scientific knowledge demands a continuous improvement of the optical resolution of the instruments. In far-field light microscopy, the attainable resolution is dictated by the limit of diffraction, which, in practice, is about 250 nm for high-numerical-aperture objective lenses. Near-field scanning optical microscopy (NSOM) was the first technique that has overcome this limit up to about one order of magnitude. Typically, the resolution range below 100 nm is accessed for biological applications. Using appropriately designed scanning probes allows for obtaining an extremely small near-field light excitation volume (some tens of nanometers in diameter). Because of the reduction of background illumination, high contrast imaging becomes feasible for light transmission and fluorescence microscopy. The height of the scanning probe is controlled by atomic force interactions between the specimen surface and the probe tip. The control signal can be used for the production of a topographic (nonoptical) image that can be acquired simultaneously. In this chapter, the principle of NSOM is described with respect to biological applications. A brief overview of some requirements in biology and applications described in the literature are given. Practical advice is focused on instruments with aperture-type illumination probes. Preparation protocols focussing on NSOM of cell surfaces and chromosomes are presented.

Key Words: Near-field scanning optical microscopy; NSOM; applications in biology; cell surfaces; metaphase chromosomes; meiotic chromosomes

1. Introduction

1.1. Diffraction Limit in Far-Field Light Microscopy

In biological settings, the usually applied microscope techniques (bright field, phase contrast, epifluorescence, confocal laser scanning, etc.) make use of the so-called far-field light microscopy. This means that the imaging process is

From: *Methods in Molecular Biology, vol. 319: Cell Imaging Techniques: Methods and Protocols*
Edited by: D. J. Taatjes and B. T. Mossman © Humana Press Inc., Totowa, NJ

determined by the physical behavior of *propagating* electromagnetic waves for specimen illumination and detection. Compared to the wavelength of light (typically in the range 400–800 nm), the distances between illumination source or detector system, respectively, and the specimen are hundreds of micrometers up to millimeters, that is they are large ("far field").

Because of the finite aperture of the microscope optics, light waves are diffracted, resulting in the well-known effect that an infinitesimal small pointlike object appears as a spread image of minimum diameter. The image intensity distribution of a pointlike object is given by the point spread function (PSF), from which a measure of spatial resolution can be defined for far-field optical microscopes ***(1)***. The classical diffraction limited optical resolution is given by

$$D = 0.61\left(\frac{\lambda}{\mathrm{NA}}\right)$$

(2,3) where λ is the wavelength of the light, NA is the numerical aperture of the objective lens, and D is the smallest distance between two pointlike objects that are imaged separately. A closely corresponding value also used as a measure of resolution is the full width at half-maximum of the PSF ***(4)***.

In addition to the physical constraints of the microscope optics, the real optical conditions of the specimen have also considerable influence on the attainable resolution in practice. Thus, in routine biological applications, the spatial resolution of far-field light microscopy is limited at about 250 nm ***(5,6)***. During the last two decades, several approaches have been described to overcome these imaging restrictions of far-field light microscopy ***(7)***. The first technique that successfully surpassed the diffraction limit has been near-field scanning optical microscopy (NSOM) (for a review, *see* **refs.** ***8*** and ***9***). Meanwhile, NSOM techniques have become a special discipline in optics, in which many laboratories develop highly sophisticated instruments and investigate their physical behavior (*see,* e.g., the 71 articles dicussed in Journal of Microscopy vol. 202, ***10***).

1.2. Principle of Near-Field Scanning Optical Microscopy

The principle of NSOM has been discovered and rediscovered several times. More than 70 yr ago, the theory of an instrument very similar in construction to modern NSOM systems was discussed ***(11)*** as a possibility for surpassing the diffraction limit of resolution ***(12)***. After the first experimental achievement of microscopic imaging with nearly atomic resolution by nonoptical scanning techniques (scanning tunneling microscopy, atomic force microscopy) ***(13,14)*** NSOM was realized ***(15,16)***.

Similar to atomic force microscopy, a sharp probe physically scans the sample surface in NSOM. The height movement of the scanning probe is controlled by the atomic force interaction between sample and probe tip, which generates

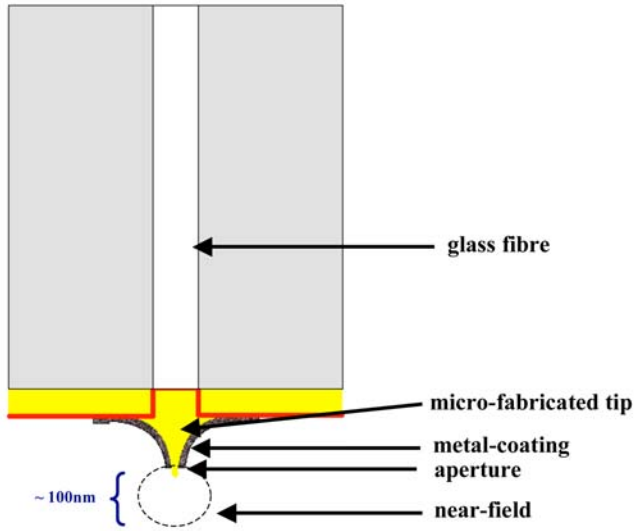

Fig. 1. Schematic representation of a NSOM probe.

a nonoptical image of the specimen topography. For biological applications, the most frequently applied NSOM probe consists of a metal (aluminum)-coated tapered optical fiber with a small aperture typically 20–130 nm in diameter at the end (*see* **Note 1**). This probe is used as a light source in optics, similar to the way the headset of a Walkman is used as a sound source in acoustics. In the latter case, the sound source has dimensions in centimeters, which is much smaller than the wavelengths of sound. Thus, the real acoustic figures and timber can only be heard if the ear is very close to the sound source (i.e., in a range much smaller than the wavelength).

In a NSOM probe tip, the incident light wave coming from a laser light source via a glass fiber is propagating into a funnel of dimensions below the diffraction limit (*see* **Fig. 1**). The light emitted by the aperture is, therefore, predominantly composed of *evanescent* waves rather than propagating waves. The intensity of evanescent waves decays exponentially with the distance from the NSOM probe tip. The region around the tip in which a significant intensity level of the evanescent wave can be detected is called the *near field* (*see* **Fig. 1**). The near-field region typically has dimensions less than 100 nm. This limits the tip-to-sample distance to considerably less than 100 nm in order to obtain high-intensity evanescent waves.

In principle, the NSOM probe tip illuminating the sample can also be used to detect the light emitted from the sample. This means that the probe tip works in the same way a doctor's stethoscope is used to detect sound generated by a lung or a heart. In this case, sound waves with a wavelength of meters are localized with an

accuracy of centimeters. Therefore, the NSOM has occasionally been termed an "optical stethoscope" ***(15)***. Nevertheless, in biological applications, near-field illumination systems are more frequent than near-field detection systems.

In the case of near-field illumination systems, the light emitted by the NSOM tip is absorbed by the sample or by fluorochromes of the sample. The light subsequently transmitted through the sample (transmitted light) or emitted by the fluorochromes (fluorescent light) is predominantly composed of propagating waves and can be collected by conventional far-field optics and sensitive detectors. However, the NSOM probe is scanning the object point by point, so that the acquired image is the result of a sequence of intensity signals obtained from each precisely localized point. Therefore, the optical resolution is determined by the size of the illumination point. Because the near-field intensity decays rapidly with the probe distance, the aperture size is an appropriate parameter for estimating the optical resolution ***(17)*** (*see* **Note 2**). According to our experience, in practice, sub-hundred-nanometer resolution is feasible for many biological applications if the aperture has a diameter of 80 nm or less.

1.3. Requirements and Applications in Biology

A NSOM image usually records a small section of a sample (typically less than 10 μm × 10 μm) with high topographic and high optical resolution (better than 100 nm). To obtain an overview of the sample and preparation conditions, it is often helpful to image the same sample with lower magnification and resolution. This requires the addition of a far-field microscope. Because image detection of NSOM is based on far-field optics, the scanning unit can be adapted to a far-field microscope, so that both imaging modes can be run with the same instrument under identical specimen conditions (*see* **Note 3**).

Near-field scanning optical microscopic imaging is a combination of topographic (atomic force) imaging and high-resolution optical (light transmission, fluorescence) imaging. Both nonoptical and optical images are acquired simultaneously. Similar to atomic force microscopy, it is essential that the probe-to-sample distance (typically in the range of 10 nm) is accurately controlled by using a force feedback loop. The optical image, however, is very sensitive to small axial movements of the tip, because the near-field illumination intensity decays exponentially with the tip-to-sample distance. Therefore, the most commonly applied control mechanism in NSOM is, in contrast to atomic force microscopy, the so-called shear-force feedback control. The NSOM probe is mounted into a piezoelectric tube so that it oscillates at its resonance frequency in a lateral vibrational mode with an amplitude typically less than 1 nm. In close proximity to the sample, the shear forces dampen this motion and induce a measurable change in the oscillation amplitude and phase, which can be used as a control signal in an electronic feedback system and for the generation of the topographic image.

The physical constraints of the shear-force feedback control require dry specimens, which seems to preclude biological applications in which a fluid environment is of central importance for structure conservation. However, structure-conserving drying procedures are known from electron microscopy *(18)* and can be modified in an appropriate way (*see also* **Subheading 3.2.**) (*see* **Note 4**). The requirement for specimen drying in NSOM fluorescence imaging imposes restrictions on the choice of fluorochromes that can be used for labeling. Furthermore, in dry samples, photobleaching might increase as a result of the direct contact with oxygen from air.

Despite these so far existing limitations, NSOM has been utilized in many applications in different fields of biology and has proven a powerful technique when surface structures or structures very near to the surface need to be visualized by means of light microscopy at high spatial resolution and contrast. So far, NSOM has, for instance, been applied for the analysis of the following:

1. Cytoskeletal actin *(19)*.
2. Green fluorescent proteins in bacteria *(20)*.
3. Cortical neurons *(21)*.
4. Membranes of erythrocytes *(22)* and skin fibroblasts *(23)*.
5. Cell surfaces of mouse fibroblasts *(24)* and lymphocytes *(25)*.
6. Cell surfaces of human breast tumor cells *(26,27)* and cardiomyocytes *(28)*.
7. Metaphase chromosomes after G-banding *(29,30)* and fluorescence *in situ* hybridization (FISH) labeling *(31–34)*.
8. Meiotic chromosomes *(33)*.
9. DNA conformation *(35,36)*.

Especially in single-molecule fluorescence studies on cells and subcellular components (e.g., single green fluorescent protein photophysics) *(19,32, 36–39)*, NSOM has a superior advantage over far-field light microscopy because the topographic (nonoptical) image simultaneously acquired with the fluorescence image allows a precise localization of the fluorescence signal on the specimen.

2. Materials

2.1. Instrumentation

1. Inverted far-field microscope with Hg-illumination system and appropriate filters for fluorescence microscopy (*see* **Notes 5** and **6**).
2. Charge-coupled device (CCD) camera and a frame grabber board (if necessary) for far-field image detection.
3. NSOM unit (*see* **Fig. 2**) implemented in the far-field microscope.
4. Motor-driven stage and sensitive detectors for light detection in near-filed imaging (photomultiplier, avalanche diode).

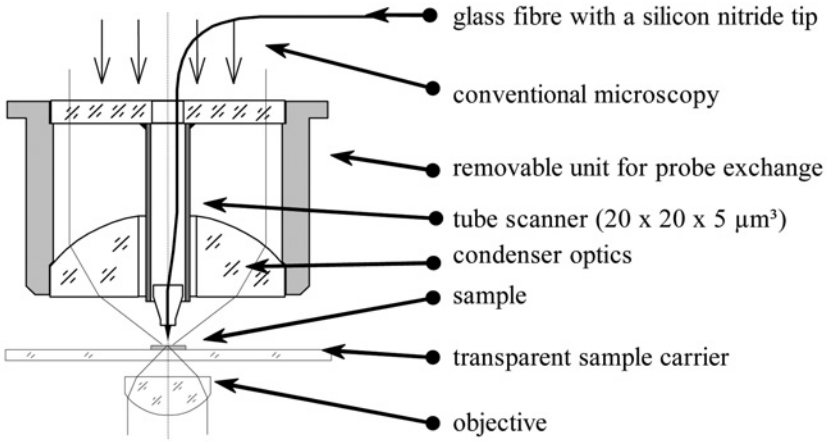

Fig. 2. Schematic representation of a NSOM unit implemented in the microscope condenser as used in a ß-type SNOM 210 from Carl Zeiss Jena (*see also* **ref**. *33*).

5. Laser module (He–Ne laser, Ar laser, etc.) with an acousto-optical tunable filter (AOTF) to select the appropriate laser wavelength and to tune the intensity.
6. Laser fiber unit to couple the light into the NSOM illumination fiber (*see* **Fig. 1**).
7. NSOM control unit.
8. Computer with software to drive the NSOM unit.
9. Image detection and evaluation software for far-field images obtained by the CCD camera.
10. Image detection and evaluation software for near-field images obtained by point detectors (optical near-field signal) and the shear-force feedback control unit (atomic force signal).

Because the aforementioned components can be obtained from various companies, we do not indicate a special brand in this section.

2.2. Solutions

1. PBS (phosphate-buffered saline).
2. 3.7% and 4% Formaldehyde prepared from fresh paraformaldehyde.
3. Ethanol (70%, 80%, 85%, 90%, 95%, 100%).
4. HMDS (hexamethyldisilazane).
5. Formamide (70%).
6. 2X SSC, 0.5X SSC (standard sodium citrate).
7. 4X SSC/0.2% Tween-20.
8. 1X PBD (phosphate-buffered detergent).
9. 10 m*M* HCl.
10. MEM medium (Life Technologies) / 0.5% mammalian protease inhibitor (Sigma).
11. 1% Lipsol.
12. Fixative I: 3.7% acid-free formaldehyde, 0.1 *M* sucrose, pH 7.4.

13. PBS/0.5% Triton X-100.
14. PBTG: PBS, 0.1% Tween-20, 0.2% bovine serum albumin (BSA), 0.1% fish gelatin.

3. Methods

3.1. Image Acquisition

The operations of the different instruments differ in many details and have to be adapted in detail to a particular setting. Therefore, the following protocol only describes essential steps. Further details have to be taken from the manufacturer's operating instructions for the given instrument.

1. Mount the NSOM probe into the NSOM unit of the microscope (*see* **Note 7**).
2. Connect the glass fiber to the laser unit and adjust the fiber so that enough light intensity is coupled into the fiber.
3. Measure the resonance frequency of the NSOM probe (*see* **Note 8**).
4. Adjust the shear-force feedback control to this frequency.
5. Move the specimen into the center of the far-field image.
6. Approach the NSOM probe to the specimen surface (*see* **Note 9**).
7. Select the field of detection.
8. Make a fast scan in order to adjust the detector gain.
9. Scan the specimen (*see* **Note 10**).

The following typical examples for the application of NSOM were performed on a SNOM 210 in the β-type version (Carl Zeiss Jena GmbH, Digital Instruments Veeco GmbH). The piezo scanning unit was integrated into the microscope condenser of an Axiovert 135 microscope. Microfabricated probes (Institut für Mikrotechnik Mainz) with silicon nitride tips coated with aluminum were mounted in a shear-force sensor support. The probes typically had an aperture of 80–100 nm. The instrument was equipped with an argon-ion laser (λ = 458 nm, 488 nm) and two He–Ne lasers (λ = 543 nm, 633 nm) for near-field illumination. The illumination intensity was tuned by an AOTF for each laser wavelength independently. Fluorescence or transmission light was detected in air by an Achroplan long-distance objective 40×/NA 0.6 and transferred to a photomultiplier or an avalanche photodiode, respectively, using appropriate filter settings. The instrument was controlled by the NanoScope IIIa controller. Further details of the instrument are described in **ref.** *33*.

3.2. NSOM of Cell Surfaces (*25,27*)

For the examples shown here (*see* **Figs. 3,4**), two types of cell systems were used:

1. Peritoneal cells (mouse lymphocytes and macrophages) dropped on glass slides.
2. Breast cancer cells of the cell line T-47D (ATCC HTB 133) (*see* **Note 11**) grown on chambered glass slides.

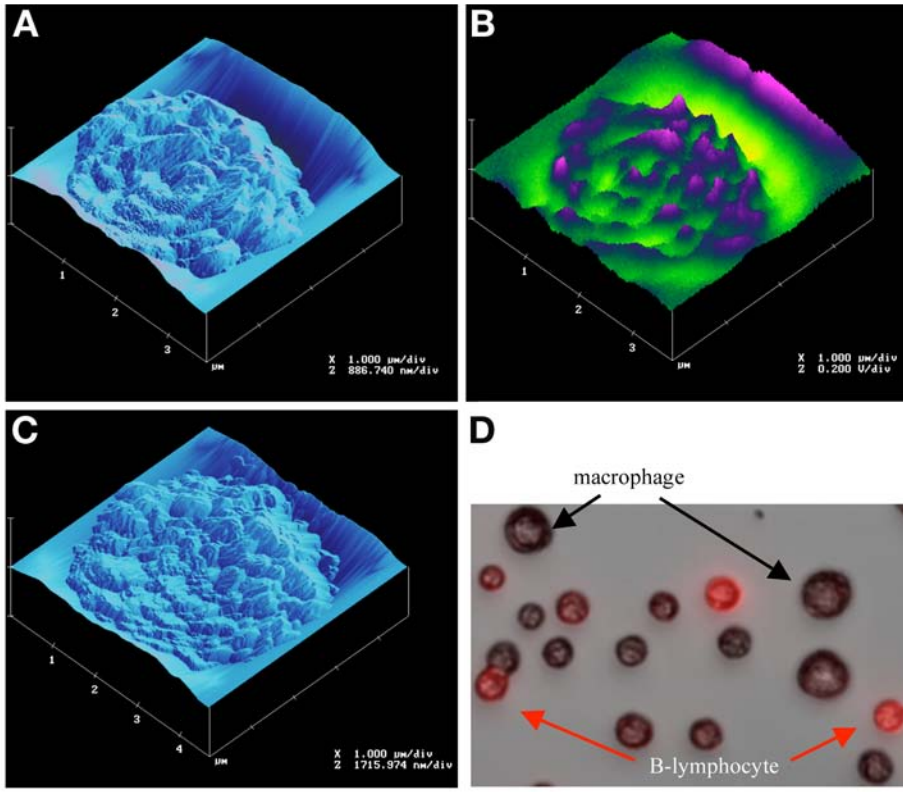

Fig. 3. NSOM images of an antibody-labeled mouse B-lymphocyte **(A**,**B)** and a mouse macrophage **(C)** of the same preparation. In the topographic images **(A**,**C)**, the different structures of the cell surfaces are visible; in the optical image **(B)**, regions of high Cy3 fluorescence intensity are shown as dark gray regions. In **(D)**, a far-field image of the same specimen is shown. The macrophages are larger than the B-lymphocytes. (Part of this figure was taken from **ref**. *25* with permission of SPIE.)

Prior to NSOM, the following preparation steps have to be done:

1. Seed and grow cells on ethanol-cleaned standard slides or cover glasses.
2. Remove cell culture medium.
3. Wash twice in PBS.
4. Fix cells with 4% formaldehyde in PBS for 15 min at 4°C.
5. Wash in PBS for 15 min at room temperature.
6. Optional: Label cell membrane with fluorescent antibodies (*see* **Note 12**).
7. Wash 15 min in PBS.
8. Dehydrate by an ethanol series (70%, 80%, 90%, 100%) at room temperature for 5 min each (*see* **Note 13**).

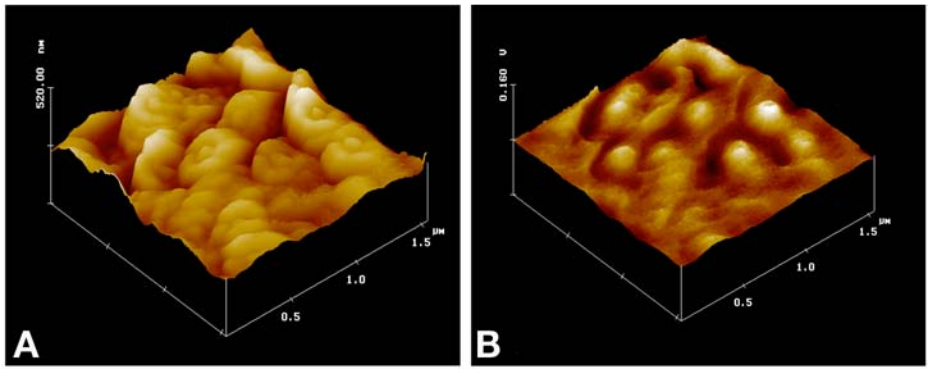

Fig. 4. Surface sections (1.5 µm x 1.5 µm) of a breast cancer cell of the line T-47D are shown. In the topographic image **(A)**, typical rosettelike cell surface structures are visible; in the optical image **(B)**, the light transmission image obtained for the He–Ne laser at 543 nm is shown (dark = high absorbance, light = high transmission). (From **ref.** *25* with permission of SPIE.)

9. Expose to HMDS (*see* **Note 13**). HMDS is known to reduce surface tension and to induce crosslinking in proteins.
10. Dry specimen at room temperature.

As an example, surfaces of peritoneal cells (mouse) (*see* **Fig. 3**) and breast tumor cells (human) (*see* **Fig. 4**) were visualized by NSOM 210. The scans were performed with a velocity of the NSOM probe of less than 1 µm/s. The images were processed (flattened, low-pass filtered) and visualized in three-dimensional topographic false color plots using the NanoScope IIIa software (version 4.42r1) running under Windows on a PC (**Figs. 3A–C** and **4**). Because the instrument is based on a standard Zeiss Axiovert microscope, far-field imaging (*see* **Fig. 3D**) was also possible using a CCD camera and a frame grabber board (Scion-Imaging). Image recording was controlled by the Scion Imaging software running under Windows on a PC.

The images obtained (*see* **Figs. 3** and **4**) show typical rosettelike and cylinderlike structures on the cell surface in the sub-hundred-nanometer range. Such studies will allow one to investigate the variations in surface morphology on a single-cell level, (e.g., after chemical or pharmacological treatment) (e.g., *27*).

3.3. NSOM of Metaphase Chromosomes After FISH (29,33,34)

Fluorescence *in situ* hybridization *(40,41)* has become a routine technique in biomedical research and clinical diagnostics. For NSOM, standard FISH techniques can be applied. However, after specific DNA labeling, the specimen has to be dried carefully, which precludes the use of certain fluorochromes in NSOM applications.

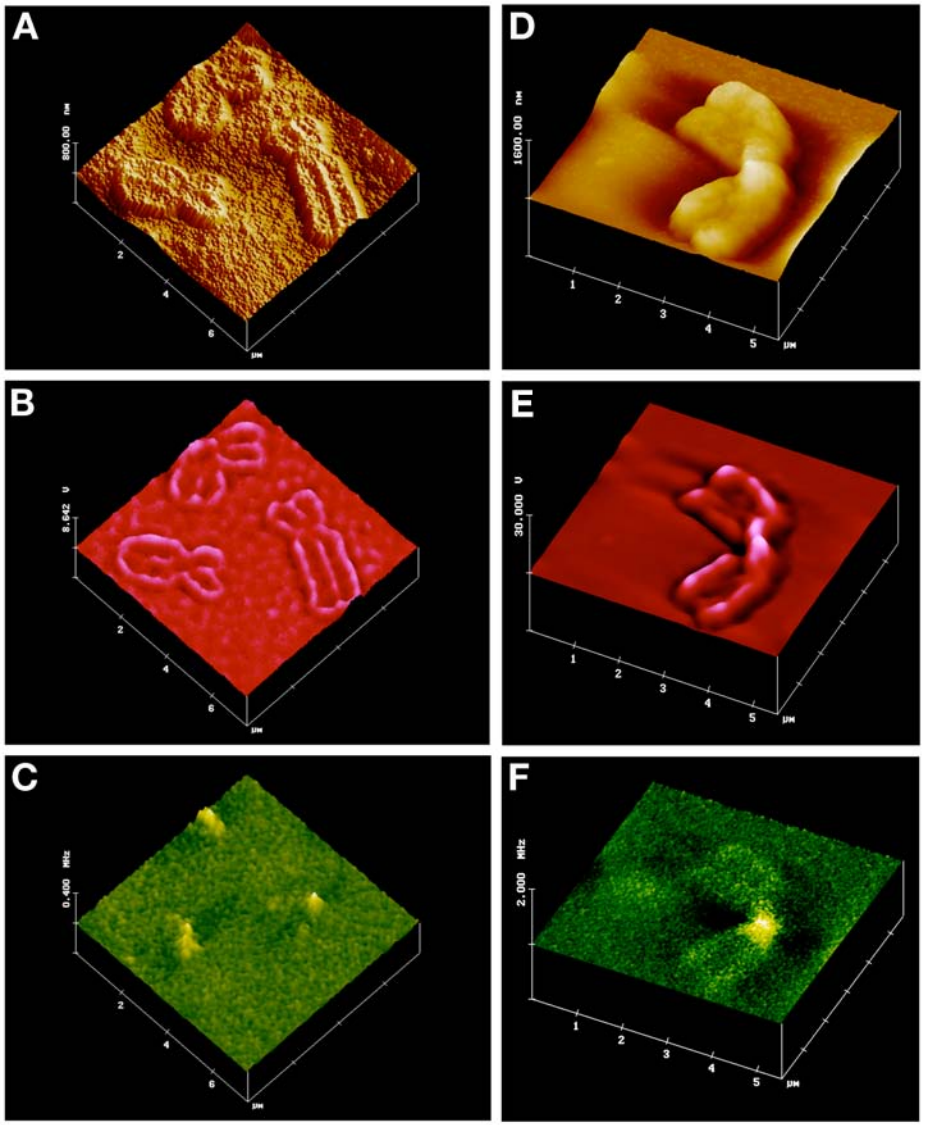

Fig. 5. NSOM images of human metaphase chromosomes after "standard" FISH **(A–C)** and low-temperature FISH **(D–F)** (*see* **ref.** *34*) with a Cy3-labeled centromeric DNA probe. **(A)** The topographic near-field image reveals that chromosome arms display a collapsed structure, particularly of the central region of the chromatids, leaving higher rims at the chromosomal border. **(B)** NSOM transmitted light image at 543 nm showing a high intensity at the chromosomal border only, which verifies the topographic impression. **(C)** NSOM fluorescence image of Cy3 fluorescence in the centromeric region detected via a 590-nm long-pass filter. The high fluorescence intensity corresponds to the absorption at

The following protocol is based on a commercially available protocol:

1. Obtain chromosome spreads by standard fixation techniques (e.g., methanol/acetic acid fixation, formaldehyde fixation, etc.) (*see* **Note 14**).
2. Prepare and label respective DNA probe and dissolve in hybridization solution according to the protocol of the manufacturer of a labelling kit of your choice (*see* **Note 15**).
3. Denature preparation in 70% formamide/2X SSC at 70°C for 2 min, and DNA probe for 3 min at 95°C.
4. Dehydrate preparations through an ethanol series (70%, 80%, 95%) at 4°C for 2 min each.
5. Add DNA probe mixture to the slide.
6. Cover the hybridization mixture and preparations with a coverglass, seal with rubber cement, and hybridize in a humidified chamber at 37°C overnight.
7. Remove the seal and coverglass.
8. Wash in 0.5X SSC (pH 7.0) at 72°C for 5 min.
9. Transfer preparations to 1X PBD at room temperature.
10. Detect the hybrid molecules by incubation with fluorochrome-labeled secondary antibodies (*see* **Note 16**).
11. Counterstaining of the chromosomes is not necessary.
12. Rinse slides three times 2 min each in 1X PBD.
13. Air-dry preparations at room temperature.

This standard FISH technique involves denaturation of the probe and target DNA at temperatures ≥70°C, thereby creating single-stranded DNA molecules that form hybrids upon reassociation of the complementary DNA sequences. A typical NSOM image series of thermally denatured metaphase chromosome preparations and specific fluorescent labeling of all centromeres by FISH is shown in **Fig. 5**. The granularity of the chromosome morphology (see **Fig. 5A–C**) indicates that thermal denaturation processes of standard FISH techniques might have detrimental effects on chromatin organization. Therefore, an alternative to standard FISH protocols was introduced that omits denaturing chemical agents and thermal treatment ("low-temperature FISH") ***(42)***. The following protocol is particularly suitable for detecting repetitive centromere probes:

1. Obtain chromosome spreads and DNA probe as described above (*see* **Note 14**).
2. Treat specimen with RNase in 2X SSC at 37°C for 1 h.

Fig. 5. *(Continued)* the centromere in (b). **(D–F)** Human metaphase chromosome 1 after visualization of the 1q12 pericentromeric region by "low-temperature" FISH using the DNA probe pUC1.77. **(D)** Topographic near-field image indicates that the FISH method applied maintains a filled appearance of the chromatids. **(E)** NSOM transmitted light image at 543 nm. High transmission is apparent along the chromatids. **(F)** NSOM fluorescence image (detected via a 590-nm long-pass filter) reveals strong signal at the hybridisation site.

3. Wash 3 min in 2X SSC at 37°C.
4. Incubate in 10 m*M* HCl for 2 min.
5. Add freshly prepared pepsin (final conc. 0.2 mg/mL) to prewarmed 0.01 *N* HCl in a Coplin jar at 37°C. Submerse preparations and incubate for 10 min.
6. Rinse the slides with distilled H_2O and wash twice in 2X SSC for 5 min.
7. Subject to a short fixation with freshly prepared 4% formaldehyde in PBS for 10 min at room temperature.
8. Wash twice again in 2X SSC.
9. Dehydrate through an ethanol series (70%, 85%, 95%) for 5 min each.
10. Air-dry preparations at room temperature.
11. Add 5 µL of the previously denatured probe mixture to the preparation and seal it with rubber cement under a plastic cover glass.
12. Hybridize for 15 h at 37°C.
13. Peel off rubber cement, float off cover glasses in 4X SSC/0.2% Tween-20 and wash preparations again for 5 min in the same solution at 37°C.
14. Incubate in 10% blocking solution in PBS or in 1.5% dry skim milk in PBS for 5 min.
15. Detect the hybrid molecules by an appropriate antibody–fluorochrome system (e.g., antidigoxigenin–Cy3 Fab fragments, or avidin–Cy3 in the case of biotin as the label of the DNA probe).
16. Wash in PBS for 10 min at room temperature.
17. Subject to another ethanol series (70%, 85%, 95%) for 5 min each.
18. Counterstaining of the chromosomes is not necessary for NSOM.
19. Air-dry the sample at room temperature.

A typical example of a metaphase chromosome after low-temperature FISH *(42)* is shown in **Fig. 5D–F**. In this case, chromosome 1 was labeled with a subcentromeric DNA probe (pUC1.77; *see* **Note 17**). The chromosome appears more voluminous with a "smooth" (i.e., less granular) surface as compared to thermal denaturation (compare **Fig. 5A**,**D**). After standard FISH, the chromosomes are generally very flat; signal and background intensities are at about the same levels. In contrast, an intensive transmitted light signal was restricted to the chromatids of the low-temperature FISH chromosomes, indicating an intensive near-field object interaction (*see* **Fig. 5E**). The fluorescence image shows a clearly visible labelling site at the centromeric region (*see* **Fig. 5F**).

3.4. NSOM of Meiotic Chromosomes (33)

Meiosis is the cell division type that contributes to sexual reproduction by reducing the diploid chromosome number to the haploid. Meiotic chromosomes display a unique organization in that they exhibit a proteinaceuos chromosome core along replicated sister chromatids, and the DNA emanates as loops from these cores. Cores of homologous chromosomes are connected during pachytene by a protein zipper called the synaptonemal complex (SC). The ends of the SCs

are capped by the telomeres, which (in addition to other aspects) play an important role in the chromosome-pairing process at first meiotic prophase. So far, little is known about the relative distribution of telomere proteins within ends of the meiotic chromosome cores. NSOM might be a means to gain a better insight into the spatial organization of the meiotic telomere. The following (for details, *see* **ref.** *43*) describes the preparation of meiotic chromosome spreads for NSOM:

1. Mince fresh or frozen testicular tissue in MEM medium/0.5% mammalian protease inhibitor (Sigma) at 4°C.
2. Remove tissue pieces and place a drop of the suspension on clean, aminosilane-coated glass slides (Super plus; Menzel Gläser).
3. Mix 50 µL of cell suspension and 150 µL of 1% Lipsol on a slide.
4. Briefly tilt the slide after each step to mix the solutions evenly within the resulting drop.
5. After 5 min, add fixative I and distribute the suspension evenly by streaking with the side of a pipet tip over the slide without touching the surface.
6. Fix specimen by adding 200 µL fixative I. Allow to air-dry in a fume hood.
7. Wash for 30 min with 0.5% Triton X-100/PBS.
8. Wash with PBS.
9. Incubate for 10 min in PBTG.
10. Incubate at 4°C overnight with 100 µL PBTG containing the primary antibody under a cover slip in a humid chamber (*see* **Note 18**).
11. Rinse three times 3 min with PBTG at 37°C.
12. Incubate for 30 min at 37°C with secondary, fluorochrome-conjugated antibody of choice (*see* **Note 19**).
13. Wash three times 3 min in PBS.
14. Dehydrate through an ethanol series (70%, 85%, 95% for 5 min each).
15. Air-dry the sample at room temperature.

For an example of successful labeling at a meiotic telomere, see **Fig. 6** and Color Plate 15, following p. 274. The meandering parts of the SC are visible in the topographic and light transmission image. From the fluorescence image, TRF2 signals can be localized in the telomere knob.

3.5. Discussion and Perspective

Many applications have shown that the intrinsic advantages of NSOM make this technique extremely useful for high-resolution imaging in life sciences. Nevertheless, it seems that NSOM is rarely applied in biology. Some features might be responsible for this situation: First, compared to far-field light microscopy, NSOM is a complex technique that requires detailed training of the operator before images of good quality can be obtained. Second, most near-field microscopes are devices in experimental physics laboratories and not widely accessible to the biologist. The commercially available instruments are primarily designed for measurements of solid-state physics and are not always

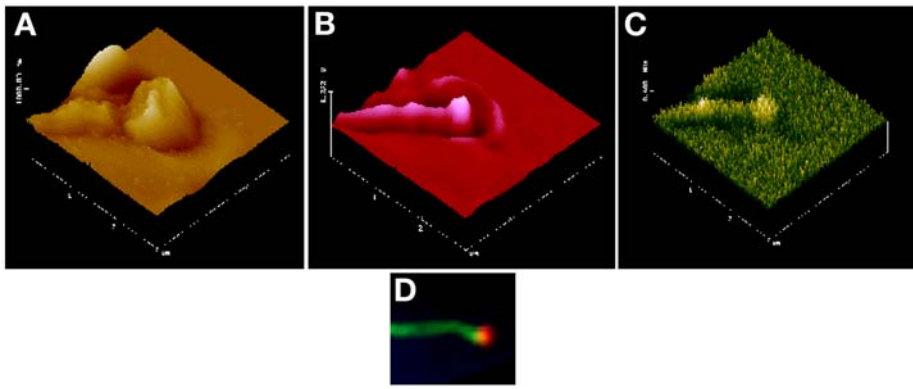

Fig. 6. NSOM images of the telomeric region of a human meiotic chromosome core after immunostaining of TRF2 by Cy3-labeled antibodies. **(A)** The topographic image shows a thickened telomere at the end of the core (called the attachment plate); **(B)** a telomeric knob as regions of higher intensity of transmitted light at 543 nm; **(C)** Cy3 fluorescence of the TRF2 antibody labeling site, which was recorded via a 590-nm low-pass filter; **(D)** far-field fluorescence image of the synaptonemal complex and the TRF2 label at the telomere (*see* Color Plate 15, following p. 274).

adapted to the requirements of biological experiments—for instance, the use of standard glass slides as specimen carrier. Third, the resolution and sensitivity of NSOM depends not only on the quality of the probe but also on the quality of the specimen. Especially, the drying process required because of the shear-force feedback control has to be done with great care in order to conserve the native supra molecular structures of the specimen. Despite great efforts of several groups ***(44–46)***, it remains a technical challenge to develop an instrument that works in a liquid (i.e., more physiological environment) and allows for near-field analysis of "soft objects."

4. Notes

1. The scanning probe is the most critical element of the complete technique. It is difficult to produce such probes in such a way that NSOM imaging can reproducibly be performed for the same specimen. Therefore, a reliable procedure to produce large quantities of high-quality probes is microfabrication of metal-coated silicon oxide or silicon nitride tips that are glued on glass fibers. However, examples of biological applications have been described using non-metal-coated aperture-type probes. Other types of probe referring to the so-called "apertureless" types are described in the literature, but, to our knowledge, they have not been applied for any routine application in biology.
2. As in far-field light microscopy, in practice the optical resolution of NSOM strongly depends on the experimental conditions applied (NSOM probe, light

intensity, optical conditions of the sample, sample topography, etc.). Structurally conserved surfaces of cells or organelles often show gross topological changes (typically several micrometers). In this case, the topography might modulate the optical signal because the axial tip-to-sample distance is not always the shortest tip-to-sample distance that controls the height movement of the NSOM probe. This effect can modulate the optical resolution within the image and could also cause artifacts in the image *(47,48)*. However, theoretical approaches exist that allow for an approximate determination of the resolution of NSOM also from images of biological samples *(49)*.

3. The combination of far-field and near-field microscopy in one instrument is an advantage for the user, especially for biological applications, if switching between both instrumentation modes can be done without changing the sample or sample carrier. Therefore, it is of practical importance in biological applications that the standard glass slides or cover glasses, which are routinely applied in far-field light microscopy, can also be used for specimen preparation under NSOM conditions.
4. The shear-force feedback control reacts also on transparent surface material. Hence, care has to be taken not to cover the specimen by some material that should not be imaged.
5. The microscope has to be protected against low-frequency vibrations of the surroundings by means of an active optical table.
6. If standard glass slides are used for far-field and near-field microscopy, long-distance objectives are useful to focus through the slide.
7. Several manufacturers offer NSOM probes. They are usually delivered ready to use for a given instrument. In all cases, special care has to be taken in handling the NSOM probe in order not to destroy the probe tip.
8. Each NSOM probe has its own resonance frequency that has to be determined after changing the NSOM probe. Sometimes more than one resonance can be detected. In this case, the frequency that displays the highest resonance amplitude should be utilized for the NSOM control.
9. By visual far-field microscopy, the NSOM probe can be manually adjusted into a focal plane above the specimen surface. The final approach of the NSOM tip should be done by the instrument under shear-force control.
10. Most biological samples are so-called soft samples (compared to solid-state surfaces) with large height modulations (typically in the micrometer range). Therefore, a very slow scan velocity is recommended (less than 1 μm/s).
11. Breast cancer cells of the cell line T-47D (ATCC HTB 133) were grown on chambered glass slides (Nalge Nunc International, Naperville, IL USA) and cultivated in RPMI 1640 cell culture medium with 10% fetal calf serum at 37°C with 5% CO_2 in a humidified atmosphere. Three to four days before reaching a confluent cell monolayer, the medium was changed to phenol red-free RPMI 1640, including 5% charcoal-stripped fetal calf serum, 1% antibiotic/antimycotic solution (GIbco BRL/Life Technologies), 2 m*M* glutamine, and 1% nonessential amino acids solution. After 6 d of further cultivation, aliquots of the cells were treated for

48 h with 17ß-estradiol (Sigma-Aldrich Chemie GmbH, Deisenhofen, Germany) at concentrations of 5×10^{-9} *M*, 5×10^{-7} *M*, or 5×10^{-5} *M*. The 17ß-estradiol stock solution was prepared in ethanol *(27)*.

12. Mouse peritoneal cells: Immunoglobulin G on the mouse lymphocytes was visualized by biotinylated goat–anti-mouse IgG antibodies and Cy3-conjugated streptavidin. The incubation time was 15 min for each step. Cy3 is well suited for NSOM because of its high photostability (*see* **Subheading 1.3.**).
13. The duration of the ethanol and HMDS exposure is very critical on the conservation of cell surface structures. The appropriate exposure times have to be tested experimentally. For the examples described here, the optimum was as follows:

	Duration of each ethanol step	Duration of HMDS exposure
Fresh peritoneal cells	2.5 min	1.0 min
Cancer cells of T-47D	5.0 min	3.0 min

14. For the experiments presented here, lymphocytes were prepared from fresh peripheral blood and stimulated with phytohemagglutinin M to grow for 72 h. The cells were synchronized and arrested in mitosis by a colcemid block for the last 2 h of cultivation. After hypotonic treatment with prewarmed KCl (75 m*M*), the cells were fixed with cold methanol/acetic acid (3:1, v/v). Metaphase chromosomes and interphase cell nuclei were spread on precleaned slides. After evaporation of the fixative, the slides were stored in 100% ethanol at 4°C. Prior to FISH, they were rinsed with 100% ethanol and air-dried.
15. A commercially available DNA probe (Appligene Oncor) specific for all centromeres was used. This probe was labeled with digoxigenin. According to the manufacturer´s instruction, 1.5 µL of probe DNA was denatured in 30 µL Oncor Hybrisol VI (containing 50% formamide) at 72°C for 5 min.
16. For detection of the hybrid molecules, 60 µL of Cy3-labeled antidigoxigenin was applied and incubated under a plastic cover slip at 37°C for 45 min.
17. A DNA probe (pUC 1.77) specific for the region q12 on chromosome 1 was used for the experiments shown in **Fig. 5D–F**. The pUC 1.77 probe was labeled with biotin-11-dUTP. Five microliters of DNA probe (about 100 ng) were diluted with 3 µL 20X SSC, 3 µL of 10X HCl-Tris, and 19 µL of H_2O and denatured at 95°C for 4 min. The hybridization solution was cooled down to approx 60°C and kept at this temperature until use.
18. To our current knowledge, the NSOM data described here and in **ref**. *33* are the very first experiments in which NSOM imaging was performed to visualize telomere proteins of meiotic chromosomes. The labeling pattern shown was obtained with different primary antibodies, such as rabbit anti-human TRF1 or rabbit anti-human TRF2 *(43)*.
19. For the detection of the primary rabbit antibodies consecutive incubations with a secondary biotinylated anti-rabbit antibody and avidin–Cy3 were performed.

The Cy3 fluorochrome proved effective in all NSOM experiments and was superior to FITC or Cy5.

Acknowledgments

Funding by the BMBF (Bundesminister für Bildung und Forschung) and the instrumental support of Carl Zeiss Jena GmbH are gratefully acknowledged. H.S. is grateful to C. Heyting, Wageningen, NL and T. de Lange, RU, New York, USA, for help with the antibodies and acknowledges support from the DFG (grant no. Sche350/8-3). The authors are indebted to J. Beuthan and C. Dressler, Berlin, for providing the breast cancer cells and for stimulating discussions. The authors thank H. Dittmar, G. Günther, B. Lanick, IMB, Jena, and M. Jerratsch, University of Kaiserslautern for technical assistance. The work of M.H. was partly supported by a NCI/CCR Intramural Research Award to S. Janz.

References

1. Abbe, E. (1873) Beiträge zur Theorie des Mikroskops und der mikroskopischen Wahrnehmung. *Arch. Mikrosk. Anat.* **9,** 413–468.
2. Lord Rayleigh, F. R. S. (1879) Investigation in optics, with special reference to the spectroscope. *Philos. Mag.* **8,** 261–274.
3. Born, M. and Wolf, E. (1970) *Principles in Optics*, 4th ed., Pergamon, Oxford, pp. 414–419.
4. Stelzer, E. H. K. (1998) Contrast, resolution, pixelation, dynamic range and signal-to-noise ratio: fundamental limits to resolution in fluorescence microscopy. *J. Microsc.* **189,** 15–24.
5. Kozubek, M. (2001) Theoretical versus experimental resolution in optical microscopy. *Microsc. Res. Tech.* **53,** 157–166.
6. Edelmann, P., Esa, A., Hausmann, M., and Cremer, C. (1999) Confocal laser-scanning fluorescence microscopy: in situ determination of the confocal point-spread function and the chromatic shifts in intact cell nuclei. *Optik* **110,** 194–198.
7. Sarikaya, M. (1992) Evolution of resolution in microscopy. *Ultramicroscopy* **47,** 1–14.
8. Zhang, P., Kopelman, R., and Tan, W. (2000) Subwavelength optical microscopy and spectroscopy using near-field optics. *Crit. Rev. Solid State Mater. Sci.* **25,** 87–162.
9. De Lange, F., Cambi, A., Huijbens, R., et al. (2001) Cell biology beyond the diffraction limit: near-field scanning optical microscopy. *J. Cell Sci.* **114,** 4153–4160.
10. Wilson, T., ed. Journal of microscopy, vol. **202,** 1–450.
11. Synge, E. H. (1928) A suggested method for extending microscopic resolution into the ultra-microscopic region. *Philos. Mag.* **6,** 356–362.
12. McCutchen, C. W. (1967) Superresolution in microscopy and the Abbe resolution limit. *J. Opt. Soc. Am.* **57,** 1190–1192.
13. Binnig, G., Rohrer, H., Gerber, C., and Weibel, E. (1982) Surface studies by scanning tunnelling microscopy. *Phys. Rev. Lett.* **49,** 57–61.
14. Binnig, G., Quate, C. F., and Gerber C. (1986) Atomic force microscope. *Phys. Rev. Lett.* **56,** 930–933.

15. Pohl, D. W., Denk, W., and Lanz, M. (1984) Optical stethoscopy: image recording with resolution λ/20. *Appl. Phys. Lett.* **44,** 651–653.
16. Betzig, E., Lewis, A., Harootuniam, A., Isaacson, M., and Kratschmer, E. (1986) Near-field scanning optical microscopy (NSOM): development and biophysical applications. *Biophys. J.* **49,** 269–279.
17. Dürig, U., Pohl, D. W., and Rohner, F. (1986) Near-field optical-scanning microscopy. *J. Appl. Phys.* **59,** 3318–3327.
18. Boyde, A. (1980) Review of basic preparation techniques for biological scanning electron microscopy, in *Electron Microscopy, Vol II* (Brederoo, P. and de Priester, W. eds.), Electron Microcopy Foundation, Leiden, pp. 768–777.
19. Betzig, E. and Chichester, R. J. (1993) Single molecules observed by near-field scanning optical microscopy. *Science* **262,** 1422–1425.
20. Subramaniam, V., Kirsch, A. K., and Jovin, T. M. (1998) Cell biological applications of scanning near-field optical microscopy (SNOM). *Cell Mol. Biol.* **44,** 689–700.
21. Talley, C. E., Cooksey, G. A., and Dunn, R. C. (1996) High-resolution fluorescence imaging with cantilevered near-field fiber optic probes. *Appl. Phys. Lett.* **69,** 3809–3811.
22. Enderle, T., Ha, T., Ogletree, D. F., Chemla, D. S., Magowan C., and Weiss, S. (1997) Membrane specific mapping and colocalization of malarial and host skeletal proteins in the *Plasmodium falciparum* infected erythrocyte by dual-color near-field scanning optical microscopy. *Proc. Natl. Acad. Sci. USA* **94,** 520–525.
23. Hwang, J., Gheber, L. A., Margolis, L., and Edidin, M. (1998) Domains in cell plasma membranes investigated by near-field scanning optical microscopy. *Biophys. J.* **74,** 2184–2190.
24. Kirsch, A. K., Subramaniam, V., Jenei, A., and Jovin, T. M. (1999) Fluorescence resonance energy transfer detected by scanning near-field optical microscopy. *J. Microsc.* **194,** 448–454.
25. Perner, B., Hausmann, M., Wollweber, L., Rapp, A., Monajembashi, S., and Greulich, K. O. (2000) Scanning near-field optical microscopy after structure conserving air-drying. *Proc. SPIE* **4164,** 10–17.
26. Nagy, P., Jenei, A., Kirsch, A. K., Szöllösi, J., Damjanovich, S., and Jovin, T. M. (1999) Activation-dependent clustering of the erbB2 receptor thyrosine kinase detected by scanning near-field optical microscopy. *J. Cell Sci.* **112,** 1733–1741.
27. Perner, B., Rapp, A., Dressler, C., et al. (2002) Variations in cell surfaces of estrogen treated breast cancer cells detected by a combined instrument for far-field and near-field microscopy. *Analyt. Cell. Pathol.* **24,** 89–100.
28. Micheletto, R., Denyer, M., Scholl, M., et al. (1999) Observation of the dynamics of live cardiomyocytes through a free-running scanning near-field optical microscopy setup. *Appl. Opt.* **38,** 6648–6652.
29. Wiegräbe, W., Monajembashi, S., Dittmar, H., et al. (1997) Scanning near-field optical microscope—a method for investigating chromosomes. *Surface Interface Anal.* **25,** 510–513.
30. Held, N., Hausmann, M., Perner, B., and Greulich, K. O. (2000) Optische Rasternahfeld-mikroskopie in der Zytogenetik. *CLB Chem. Labor Biotechn.* **51,** (9/2000), 324–327.

31. Moers, M. H. P., Kalle, W. H. J., Ruiter, A. G. T., et al. (1996) Fluorescence in situ hybridization of human metaphase chromosomes detected by near-field scanning optical microscopy. *J. Microsc.* **182,** 40–45.
32. Meixner, A. J. and Kneppe, H. (1998) Scanning near-field optical microscopy in cell biology and microbiology. *Cell. Mol. Biol.* **44,** 673–688.
33. Hausmann, M., Perner, B., Rapp, A., Scherthan, H., and Greulich, K. O. (2001) SNOM imaging of mitotic and meiotic chromosomes. *Eur. Microsc. Anal.* **71,** (5/2001), 5–7.
34. Winkler, R., Perner, B., Rapp, A., et al. (2002) Labelling quality and chromosome morphology after low temperature FISH analysed by scanning far-field and scanning near-field optical microscopy. *J. Microsc.* **209,** 23–33.
35. Ha, T., Enderle, T., Ogletree, D. F., Chemla, D. S., Selva, P. R., and Weiss, S. (1996) Probing the interaction between two single molecules: fluorescence resonance energy transfer between a single donor and a single acceptor. *Proc. Natl. Acad. Sci. USA* **93,** 6264–6268.
36. Garcia-Parajo, M. F., Veerman, J. A., Ruiter, A. G., and van Hulst, N. F. (1998) Near-field optical and shear-field microscopy of single fluorophores and DNA molecules. *Ultramicroscopy* **71,** 311–319.
37. Ambrose, W. P., Affleck, R. L., Goodwin, P. M., et al. (1995) Imaging of biological molecules with single molecule sensitivity using near-field scanning optical microscopy. *Exp. Tech. Phys.* **41,** 237–248.
38. Garcia-Parajo, M. F., Veerman, J. A., Segers-Nolten, G. M., de Grooth, B., Greve, J., and van Hulst, N. F. (1999) Visualising individual green fluorescent proteins with a near-field optical microscope. *Cytometry* **36,** 239–246.
39. Van Hulst, N. F., Veerman, J. A., Garcia-Parajo, M. F., and Kuipers, L. (2000) Analysis of individual (macro)molecules and proteins using near-field optics. *J. Chem. Phys.* **112,** 7799–7810.
40. Clark, M. (ed.) (1996) *In Situ Hybridization.* Chapman & Hall, Weinheim.
41. Van der Ploeg, M. (2000) Cytochemical nucleic acid research during the twentieth century. *Eur. J. Histochem.* **44,** 7–42.
42. Durm, M., Haar, F. -M., Hausmann, M., Ludwig, H., and Cremer, C. (1997) Non-enzymatic, low temperature fluorescence in situ hybridization of human chromosomes with a repetitive α-satellite probe. *Z. Naturforsch.* **52c,** 82–88.
43. Scherthan, H., Jarratsch, M., Li, B., et al. (2000) Mammalian meiotic telomeres: protein composition and redistribution in relation to nuclear pores. *Mol. Biol. Cell* **11,** 4189–4203.
44. Lambelet, P., Pfeffer, M., Sayah, A., and Marquis-Waible, F. (1998) Reduction of tip–sample interaction forces for scanning near-field optical microscopy in a liquid environment, *Ultramicroscopy* **71,** 117–121.
45. Mannelquist, A., Iwamoto, H., Szabo, G., and Shao, Z. (2001) Near-field optical microscopy with a vibrating probe in aqueous solution. *Appl. Phys. Lett.* **78,** 2076–2078.
46. Mannelquist, A., Iwamoto, H., Szabo, G., and Shao, Z. (2002) Near-field optical microscopy in aqueous solution: implementation and characterization of a vibrating probe. *J. Microsc.* **205,** 53–60.

47. Hecht, B., Bielefeldt, H., Inouye, Y., and Pohl, D. W. (1997) Facts and artifacts in near-field optical microscopy. *J. Appl. Phys.* **81,** 2492–2498.
48. Kalkbrenner, T., Graf, M., Durkan, C., Mlynek, J., and Sandoghdar, V. (2000) High-contrast topography-free sample for near-field optical microscopy. *Appl. Phys. Lett.* **76,** 1206–1208.
49. Beuthan, J., Hausmann, M., Minet, O., Perner, B., Dressler, C., and Eberle, H. G. (2001) Approximative determination of the modulation transfer function of the scanning near field microscope using biological samples. *Techn. Messen.* **3/2001,** 127–130.